

## Article

# Niger Seed Oil-Based Biodiesel Production Using Transesterification Process: Experimental Investigation and Optimization for Higher Biodiesel Yield Using Box–Behnken Design and Artificial Intelligence Tools

Srikanth Holalu Venkataramana <sup>1</sup>, Kanchiraya Shivalingaiah <sup>2</sup>, Mahesh Basetteppa Davanageri <sup>3</sup>, Chithirai Pon Selvan <sup>4</sup>, Avinash Lakshmikanthan <sup>5</sup>, Manjunath Patel Gowdru Chandrashekarappa <sup>6,\*</sup>, Abdul Razak <sup>7</sup>, Praveena Bindiganavile Anand <sup>5</sup> and Emanoil Linul <sup>8,\*</sup>

- <sup>1</sup> Department of Aeronautical Engineering, Nitte Meenakshi Institute of Technology, Visvesvaraya Technological University, Bangalore 560064, India; srikanth.hv@nmit.ac.in
  - <sup>2</sup> Department of Mechanical Engineering, Government Engineering College, Visvesvaraya Technological University, Hassan 573201, India; kanchirayas@gmail.com
  - <sup>3</sup> Department of Mechanical Engineering, Graphic Era (Deemed to be University), Dehradun 248002, India; coe@geu.ac.in
  - <sup>4</sup> School of Science and Engineering, Curtin University, Dubai 345031, United Arab Emirates; pon.selvan@curtindubai.ac.ae
  - <sup>5</sup> Department of Mechanical Engineering, Nitte Meenakshi Institute of Technology, Visvesvaraya Technological University, Bangalore 560064, India; avinash.l@nmit.ac.in (A.L.); praveena404@gmail.com (P.B.A.)
  - <sup>6</sup> Department of Mechanical Engineering, PES Institute of Technology and Management, Visvesvaraya Technological University, Shivamogga 577204, India
  - <sup>7</sup> Department of Mechanical Engineering, P. A. College of Engineering, Visvesvaraya Technological University, Mangaluru 574153, India; abdul\_mech@pace.edu.in
  - <sup>8</sup> Department of Mechanics and Strength of Materials, Politehnica University Timisoara, 300222 Timisoara, Romania
- \* Correspondence: manju09mpm05@gmail.com (M.P.G.C.); emanoil.linul@upt.ro (E.L.); Tel.: +91-984-485-9032 (M.P.G.C.); +40-728-44-0886 (E.L.)



**Citation:** Venkataramana, S.H.; Shivalingaiah, K.; Davanageri, M.B.; Selvan, C.P.; Lakshmikanthan, A.; Chandrashekarappa, M.P.G.; Razak, A.; Anand, P.B.; Linul, E. Niger Seed Oil-Based Biodiesel Production Using Transesterification Process: Experimental Investigation and Optimization for Higher Biodiesel Yield Using Box–Behnken Design and Artificial Intelligence Tools. *Appl. Sci.* **2022**, *12*, 5987. <https://doi.org/10.3390/app12125987>

Academic Editor: Jun Cong Ge

Received: 21 May 2022

Accepted: 9 June 2022

Published: 12 June 2022

**Publisher's Note:** MDPI stays neutral with regard to jurisdictional claims in published maps and institutional affiliations.



**Copyright:** © 2022 by the authors. Licensee MDPI, Basel, Switzerland. This article is an open access article distributed under the terms and conditions of the Creative Commons Attribution (CC BY) license (<https://creativecommons.org/licenses/by/4.0/>).

**Abstract:** The present work aims at cost-effective approaches for biodiesel conversion from niger seed (NS) oil by employing the transesterification process, Box–Behnken design (BBD), and artificial intelligence (AI) tools. The performances of biodiesel yield are reliant on transesterification variables (methanol-to-oil molar ratio M:O, reaction time Rt, catalyst concentration CC, and reaction temperature RT). BBD matrices representing the transesterification parameters were utilized for experiment reductions, analyzing factor (individual and interaction) effects, deriving empirical equations, and evaluating prediction accuracy. M:O showed a dominant effect, followed by CC, Rt, and RT, respectively. All two-factor interaction effects are significant, excluding the two interactions (Rt with RT and M:O with RT). The model showed a good correlation or regression coefficient with a value equal to 0.9869. Furthermore, the model produced the best fit, corresponding to the experimental and predicted yield of biodiesel. Three AI algorithms were applied (the big-bang big-crunch algorithm (BB-BC), firefly algorithm (FA), and grey wolf optimization (GWO)) to search for the best transesterification conditions that could maximize biodiesel yield. GWO and FA produced better fitness (biodiesel yield) values compared to BB-BC. GWO and FA experimental conditions resulted in a maximum biodiesel yield equal to  $95.3 \pm 0.5\%$ . The computation time incurred in optimizing the biodiesel yield was found to be equal to 0.8 s for BB-BC, 1.66 s for GWO, and 15.06 s for FA. GWO determined that the optimized condition is recommended for better solution accuracy with a slight compromise in computation time. The physicochemical properties of the biodiesel yield were tested according to ASTM D6751-15C; the results are in good agreement and the biodiesel yield would be appropriate to use in diesel engines.

**Keywords:** niger seed oil; transesterification process; yield; BB-BC; GWO; FA; BBD

## 1. Introduction

Energy is the dominant sector that stimulates the economy (in terms of growth, progressive development, societal status, and national security) of all countries [1,2]. Energy fulfills the basic need (food, light), necessary health care systems (vaccines, intensive care, and controlled temperature-monitoring medical equipment), educational aids (computer, television, Internet-based information transfer such as email, world-wide-web, virtual meetings, and so on), and serves as fuel for productive activities in industry, transport, agriculture, manufacturing, mining, and so on [3–5], to meet the rapid growth in population. Corresponding British Petroleum statistics on the world's energy supplies (BP2020) indicate that fossil fuels (raw oil, coal, and natural gas ~33.1%, 27%, and 24.2%) showed maximum contributions, followed by nuclear, hydro, and other renewable sources by 4.3%, 6.4%, and 5%, respectively [6]. High consumption of fossil fuels to meet strict energy demand has led to climate change that could result in global warming [7,8]. To meet energy demand and meet stricter pollution standards, researchers around the world have been drawn to identify alternate sources of sustainable and environmentally friendly fuels, such as biodiesel, ethanol, and butanol [9,10]. Biodiesel and ethyl alcohol are produced using raw materials that are generally considered renewable, mainly from plant and animal feedstocks [11]. The performance of biodiesel and ethyl alcohol in internal combustion engines has led to better engine performance and better emission characteristics [12,13]; therefore, efficient methods for the production of biodiesel from various resources or raw materials are of practical or relevant relevance.

The production of biodiesel can be achieved via pyrolysis, dilution, microemulsion, and transesterification (alkali-catalyzed, supercritical, chemistry, lipase, etc.) processes [14–18]. Transesterification is the most dominant method of biodiesel production, in which it undergoes a reaction (using the catalytic hardening reaction and yield, while a non-catalytic reaction ensures a lower yield with potential high temperature and pressure requirement) of fatty acid or oil with alcohol esters and glycerol as a result [18]. Biodiesel production is performed by the transesterification of triglycerides (containing ~10% of the incorporated oxygen fraction) that allows for the efficient combustion of fuel [19]. Many investigations have been conducted for biodiesel production utilizing various feedstocks such as Palm [20], Mahua-sunflower [21], rapeseed [22], moringa oleifera [23], Karanja [24], *Garcinia Gummi-Gutta* [25], waste fish oil, bitter almond oil, and waste cooking oil [13]. The biodiesel conversion of plant oils (*Moringa oleifera* and palm oils) and animal fats in the presence of homogeneous or heterogeneous catalysts (calcium hydroxide, NaOH, KOH) are performed with the assistance of the transesterification process [15,20,23]. The following observations are made from the analysis of the literature review that: (a) transesterification has proven to be an efficient technique for the synthesis of biodiesel using various raw materials; (b) raw materials are region-specific, which prevents demand from meeting global requirements for biodiesel production; (c) transesterification parameters need to be optimized that influence the yield of biodiesel from raw materials. Attempts are needed to select locally available and economical raw materials and to optimize transesterification parameters that could result in low-cost biodiesel.

NS oil has proven to be a potential raw material for biodiesel synthesis due to its better fuel properties [26]. NS can be cultivated in abundance in hilly, non-arable, marginal areas of India and thus treated as a viable alternative to fossil fuel [27]. Thereby, NS is available at a low cost and is used as a potential raw material for biodiesel production, in which NS-based biodiesel has been used as a potential replacement fuel for compression ignition engines [26,28]. NS is a non-edible oil seed (constituting ~37–50% oil content) grown largely in Ethiopia and India, and on a low scale in different regions in Asia, America, and Africa [29,30]. Unless the seeds are plucked from plants, they are currently used for

bird feeding in many countries [31]. The plants are grown in a low acidic, wide range of less fertile (waste area) soil conditions, roadsides, coastal areas, and so on [32]. NS oil possesses medicinal value, which acts as a partial replacement for olive and sesame seed oil utilized in pharmaceutical industries [33]. Furthermore, the byproducts are used as personal care products (soaps, perfume, etc.). NS contains higher oil content that could offer better protein and nutrition [32]. Niger plants offer flowers in July and collectible seeds in August. Niger seeds yield ~200–300 kg/hectare from plants. Niger seed contains higher fatty acids, possessing 75–80% linoleic acid and 7–8% stearic and palmitic acids [34]. Indian varieties had 25% oleic acid and 55% linoleic acid. The niger-seed-based feedstock contains free fatty acid (FFA), whose composition and acid value are estimated before applying the transesterification process. For biodiesel production, the acid or alkali catalyst transesterification process is often advantageous, wherein an oil containing triglycerides reacts faster with alcohol at a low cost without a high amount of heat requirement [35]. Higher values of free fatty acids and acids result in saponification, which deactivates the catalyst, leading to soap formation and thereby reducing the biodiesel yield [36]; therefore, the determination of free fatty acid and an acid value of oil is indeed essential before the initiation of the transesterification process. It was observed from the above literature review that not much research effort is being made to maximize the biodiesel yield from niger seed oil via the transesterification process.

The attempt to optimize the biodiesel yield for various raw materials processed through the transesterification process is presented in Table 1. Response surface methodology (RSM) based on central composite design and BBD were applied to maximize biodiesel yield after determining the optimal set of transesterification variables. It should be noted that the use of used cooking oil reduces the process costs by 60–70% [37]. The authors [37,38] applied the central composite rotatable design (CCRD) for experimentation and analysis unless practical constraints dictate that the rotatable design should not be used for experimentation and analysis [39]. Catalyst concentration was determined to be the dominant factor in the transesterification process towards conversion to biodiesel yield [40–42]. The reaction temperature showed a significant impact on biodiesel production [35,43,44]. The methanol ratio was identified as an important factor contributing to the conversion of biodiesel yield [45,46]. It has been observed that the KOH catalyst has led to a higher conversion of biodiesel than that obtained for the CaO catalyst [47,48]. Note that the catalyst concentration is the most important contributing factor for the KOH catalyst, whereas the most important contributing factor was reaction time for the CaO catalyst during the conversion of waste cotton-seed cooking oil to biodiesel [47]. From the analysis of the above literature, it was observed that, although many experiments and optimization of transesterification parameters were performed, the optimal conditions and influence of the parameters on biodiesel yield are different from each other. This is due to the existing collective differences in the raw material and their properties. Furthermore, CCD and BBD based on RSM is an effective statistical technique for enhancing the transesterification technique that could maximize biodiesel conversion [49]. Furthermore, CCD requires more experimental trials and more computation effort, time, and cost than BBD [35,42,48,50].

**Table 1.** Biodiesel production via transesterification process utilizing various feedstocks.

Feedstock	Catalyst	Process Parameters	Optimization	Major Results	Ref.
Castor oil	KOH	Rt: 30–150 min, CC: 0.5–2 wt.%, RT: 50–70 °C, OMMR: 1:3–1:9	CCD and RSM	94.9% yield	[51]
Musa acuminata peduncle	CRBP	CC: 1.5–3.5 wt.%, OMMR: 6–14, Rt: 40–120 min	CCD and RSM	98.73% yield	[41]
Waste cooking oil	NaOH	OMVR: 0.1–1, Rt: 10–60 s, MP: 100–400 w	CCRD and RSM	94.6% yield	[37]
Rubber seed oil	RSS	Rt: 60–70 min, CC: 2.5–3.5 g, OMMR: 0.2–0.3	CCD and RSM	80% yield	[40]

Table 1. Cont.

Feedstock	Catalyst	Process Parameters	Optimization	Major Results	Ref.
Soybean oil	NaOH	Rt: 60–100 min, CC: 0.5–1.3 wt.%, RT: 50–70 °C, MR: 6:1–12:1	CCRD and RSM	NR	[38]
Waste cooking oil	Sulfated zirconia	Rt: 30–120 min, CC: 2–4 wt.%, RT: 90–150 °C, OMMR: 9:1–21:1	CCD and RSM	93.5% yield	[43]
Flaxseed oil	KOH	Rt: 30–60 min, CC: 0.4–1 wt.%, RT: 35–65 °C, MR: 4:1–6:1	CCD and RSM	98% yield	[45]
Pithecellobium dulce seed oil	KOH	Rt: 60–120 min, CC: 0.4–1.2 wt.%, RT: 55–65 °C, MR: 1:3–1:9	BBD and RSM	93.24% yield	[35]
Waste cooking oil-Calophyllum inophyllum oil	KOH	Rt: 2–10 min, CC: 0.4–1 wt.%, SS: 600–1000 rpm, OMMR: 9:1–21:1	BBD and RSM	98.3% yield	[50]
Camelina oil	KOH	Rt: 5–8 min, CC: 0.5–1.5 wt.%, MRAO: 9:1–21:1	BBD and RSM	95.31% yield	[42]
Waste cotton-seed cooking oil	KOH	M:O: 6–10, CC: 0.3–0.7 wt.%, Rt: 6–12 min	FFD and RSM	96.77% yield	[47]
Waste cotton-seed cooking oil	CaO	M:O: 8–12, CC: 0.5–2 wt.%, Rt: 6–12 min		90.5% yield	
	KOH	M:O: 4.5–7.5, CC: 0.3–0.7 wt.%, RT: 40–60 °C	BBD and RSM	97.76% yield	[48]
Kapok (Ceiba pentandra) oil	CaO	M:O: 6–12, CC: 0.5–1.5 wt.%, RT: 6–12 °C		96.16% yield	
	Immobilized lipase	M:O: 4–20, WC: 2–22 vol.%, RT: 30–40 °C	CCD and RSM	96.4% yield	[52]
Olive oil	KOH	M:O: 3–15, CC: 0.4–2 wt.%, PL: 100–900 W, Rt: 3–15 min	Try-error-method	93.5% yield	[53]
Almonds of Syagrus cearensis	H <sub>2</sub> SO <sub>4</sub> + KOH	M:O: 6–60, CC: 1–5 wt.%, Rt: 10–30 min	FFD and RSM	99.99% yield	[54]
Rubber seed oil	H <sub>2</sub> SO <sub>4</sub>	AOMR: 6–15, CC: 0.5–10.5 wt.%, Rt: 50–90 min, RT: 50–70 °C	BBD and RSM	75.4% yield	[55]
Acai seeds and refined soybean oil	Acai seed ash catalyst	AOMR: 6–24, CC: 3–15 wt.%, Rt: 60–300 min, RT: 60–120 °C	CCD and RSM	98.5% yield	[44]
Palm oil	Zn-Ce/Al <sub>2</sub> O <sub>3</sub>	M:O: 12–24, CC: 5–10 wt.%, RT: 58–72 °C	CCD and RSM	87.4% yield	[47]
Pig and neem seed	CaO	M:O: 12–24, CC: 2–4 g, Rt: 50–70 min, RT: 50–60 °C	CCD and RSM	98.05% yield	[56]

AOMR: alcohol to methanol oil ratio, CL: catalyst loading, CCRD: central composite rotatable design, KOH: potassium hydroxide catalyst, MP: microwave power, MR: molar ratio, MRAO: methanol ratio of alcohol to oil, NaOH: sodium hydroxide, OMMR: oil-to-methanol molar ratio, OMVR: oil-to-methanol volume ratio, PDSO: Pithecellobium dulce seed oil, RSM: response surface methodology, RSS: rubber seed shell, SS: stir speed.

Transesterification parameters (M:O, ripe plantain fruit peel catalyst, reaction temperature, and time) that were optimized via an artificial neural network integrated with a genetic algorithm (ANN-GA) technique resulted in a maximized yield of 99.2% [57]. GA was applied to convert the microalgae oil to biodiesel yield (98.12%) subjected to optimizing the transesterification parameters (Rt, RT, and M:O) [58]. ANN models predicted the thermal conductivity of Al<sub>2</sub>O<sub>3</sub>-Cu/EG and nano-antifreeze applications [59,60]. ANN performed better than the RSM model in predicting the yield of soybean biodiesel [61], palm kernel oil biodiesel [62], sesame oil biodiesel [63], and so on. The reason for better performance by artificial intelligence tools than RSM is summarized as follows [64,65]: (a) Experimental data specified as per the predefined design matrix by RSM result in poor generalizability for unknown factors, and the model does not perform global optimization. RSM does not have good generalizability for unknowns and the model cannot conduct global optimization, as experimental data are defined according to the initial design matrix. (b) AI tools predict unknown data from a known set of data due to better generalizability with the essence of intelligence that establishes a system capable of responding identically to those performed by human intelligence. (c) Traditional RSM uses a deterministic search procedure with predefined rules, wherein deriving optimal solutions for multi-modal input behavior may result in local solutions. The aforementioned reasons made artificial intelligence tools outperform RSM-based optimization techniques in distinguished applications of the squeeze casting process [64], turning process [66], abrasive water jet machining [67],

wire electric discharge machining [68], CNC turning process [69], and drilling process [70]; therefore, AI tools can be used to optimize the process.

NS oil-based biodiesel poses better performance and emission characteristics in compression ignition engines [27] using NS oil-based feedstock. The above literature portrays some of the works on the optimization of production parameters using RSM that were reported with their efficacy in the production of biodiesel yield. It was understood that biodiesel yield is found to be different when a different contribution of transesterification parameters was observed. Furthermore, the highest biodiesel conversion from the feedstock is dependent truly on transesterification parameters. Niger seeds are grown in non-arable soil with low fertility soil across hilly regions, which ensures low-cost feedstock for biodiesel production. Not many research efforts have been made to use niger seeds as a potential low-cost feedstock and optimize the transesterification parameters for conversion to higher biodiesel yield. Furthermore, BBD limits more practical experiments that could provide detailed insights into a process that was not applied for biodiesel conversion from NS oil. In addition, no significant works have been reported regarding the use of artificial intelligence tools in supporting the optimization of biodiesel yield using the BBD technique.

In the present work, we attempted to study, analyze, and optimize the transesterification parameters (KOH catalyst concentration, methanol-to-oil molar ratio, reaction time, and temperature) for higher biodiesel yield from the niger-seed-based feedstock. Experiments were conducted according to the set of matrices of Box–Behnken design. Statistical analysis (main effect parameters, surface plots, regression equations, and model adequacy) was performed using RSM to analyze the parameters corresponding to the transesterification process. Optimizing transesterification parameters for higher biodiesel yield are of industrial relevance that results in reduced cost and time incurred in the production of biodiesel. Artificial intelligence tools (BB-BC, GWO, and FA) were applied to determine the optimized condition based on the regression equations derived based on experimental data collected using BBD and analyzed based on RSM. The performances of the three algorithms were tested based on solution accuracy and computation time. The physicochemical characteristics of biodiesel yield were studied as per ASTM D6751 standards to examine the performances of fuel properties suitable for diesel engines.

## 2. Materials and Methods

### 2.1. NS Origin and Features

For the present work, niger seeds are procured from a local Bangalore store. Oil extraction was achieved via a mechanical expeller. To separate moisture from the extracted oil, it was purified and later roasted at 110 °C. Sigma-Aldrich, India provided the chemical reagents (methyl alcohol, potassium hydroxide, and sulfuric acid) required for the transesterification process. Figure 1 explain the framework employed for biodiesel conversion from NS oil.

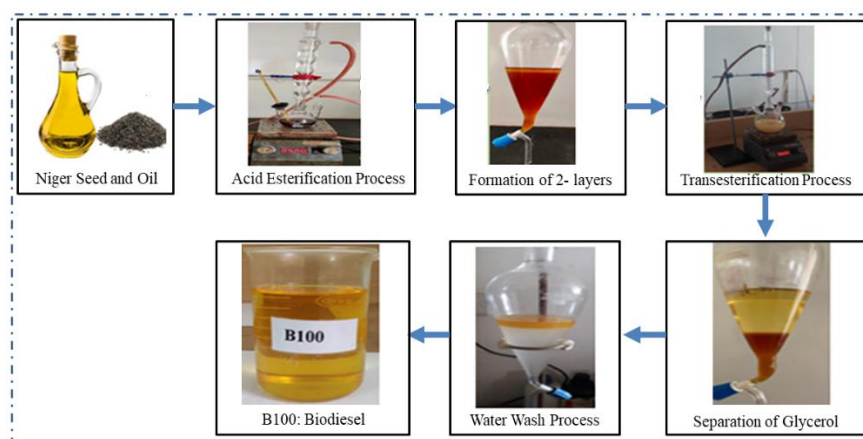


**Figure 1.** Framework for biodiesel conversion from niger seed oil.

## 2.2. Biodiesel Production and Its Characterization

### 2.2.1. Free Fatty Acid and Acid Value of Niger Seed Oil

FFA and acid values corresponding to NS oil were found to be 7% and 14 mg KOH/g, respectively. Acid-catalyzed esterification followed by a base-catalyzed transesterification process was employed. At 50 °C, for two hours with steady stirring, the esterification reacted with H<sub>2</sub>SO<sub>4</sub> (3 v/v%) and 35 (v/v%) methanol. The obtained product, after the 1-step transesterification process, was tested for acid value and was found to equal 1.5 mg KOH/g and was thus treated using the base-catalyzed transesterification process. The acid-catalyzed parameters were fixed after conducting a few pilot experimental trials in a research laboratory.

### 2.2.2. Design and Optimization of a Base-Catalyzed Transesterification Method

Figure 2 explains the framework of the proposed research work used for the conversion of NS oil to high-yield biodiesel. RSM is a collection of statistical and mathematical techniques that could determine the perspectives of the process (terms: linear, square, and interaction variables) according to the CCD and BBD experimental matrices [71]. The points (BBD focuses on middle-level experiments and CCD focuses on corner-level experiments) considered in design space were often different for the two models (BBD and CCD) and thus resulted in a difference in polynomials (e.g., coefficients, fits, and significance) [64,72]. BBD was employed in the present work for experimentation; an analysis of biodiesel yield is presented in Table 2.

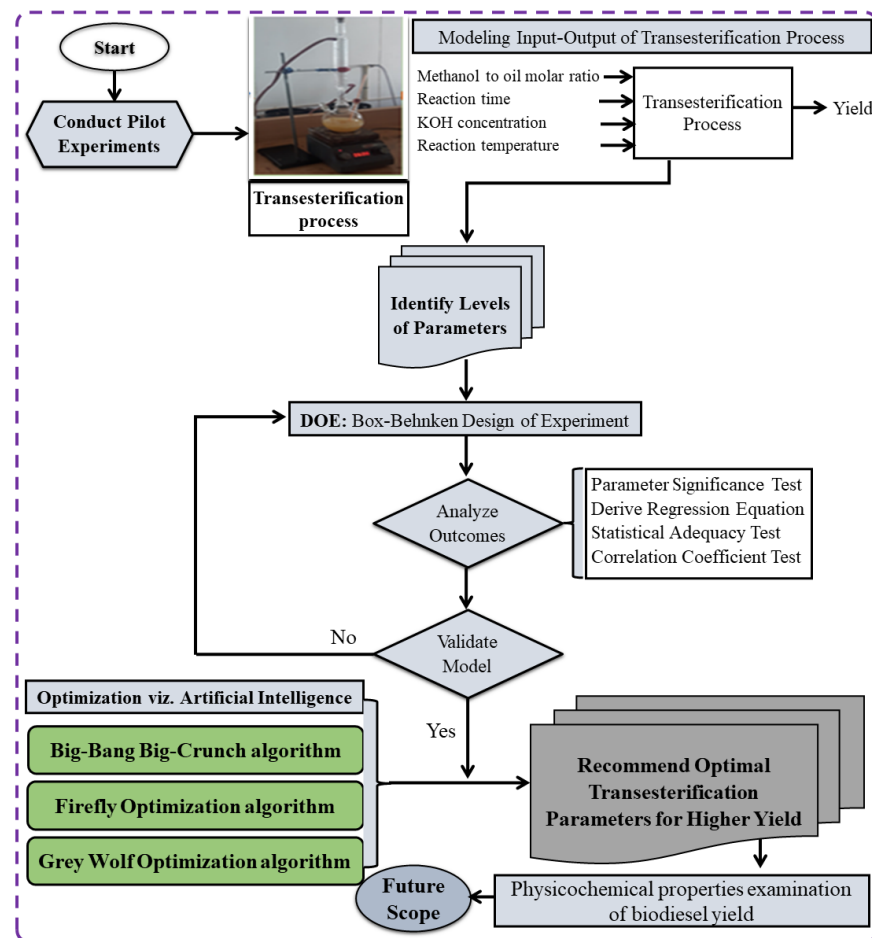


Figure 2. Framework for modeling and optimization for higher biodiesel yield.

**Table 2.** Transesterification parameters and operating levels.

Symbols	Factors	Levels		
		Low	Medium	High
A	Methanol-to-oil molar ratio	3	7.5	12
B	Catalyst concentration (wt.%)	0.5	1.0	1.5
C	Reaction temperature (°C)	50	57.5	65
D	Reaction time (min)	60	90	120

The experimental matrix corresponding to the Box–Behnken design (BBD) is defined according to Equation (1).

$$\text{No. of Experiments} = 2 \times \text{No. of independent variables} (\text{No. of independent variables} - 1) + \text{Center points} \quad (1)$$

In the present work, four independent variables and five center point experiments were considered in our experimentation. Table 3 displays the results of 29 experimental trials. Each experiment was repeated thrice, and the average values corresponding to yield were recorded. The Design-Expert software, version 11, was used to define the experimental matrix and perform statistical analysis. After each experimental run, the biodiesel samples were permitted to settle in a separate sieve for approximately twelve hours. Note that the samples were separated, with methyl esters appearing on the apex and glycerol settling at the bottom of the funnel. To eliminate the water content in the biodiesel, the resulting methyl esters were water-washed and warmed to a high temperature. The steps involved in converting NS oil-to-biodiesel yield using the transesterification process are explained in Figure 1.

**Table 3.** BBD matrix-based experimental input–output data collection of the transesterification process.

Run	A: Methanol-to-Oil Molar Ratio	B: Catalyst Concentration (wt.%)	C: Reaction Temperature (°C)	D: Reaction Time (min)	Experimental Biodiesel Yield (%)	Predicted Biodiesel Yield (%)
1	7.5	1.5	57.5	60	92.5 ± 0.4	91.3
2	12.0	1.0	57.5	60	89.0 ± 0.8	88.8
3	3.0	1.0	57.5	60	87.0 ± 0.6	86.9
4	7.5	0.5	57.5	60	87.0 ± 0.3	87.3
5	7.5	1.0	50.0	60	90.5 ± 0.4	90.4
6	7.5	1.0	65.0	60	91.7 ± 0.7	91.8
7	12	1.5	57.5	90	91.0 ± 0.5	90.9
8	7.5	1.0	57.5	90	92.0 ± 0.4	91.6
9	3.0	0.5	57.5	90	85.5 ± 0.2	85.7
10	7.5	0.5	65.0	90	89.1 ± 0.4	88.5
11	12	0.5	57.5	90	85.5 ± 0.3	85.4
12	7.5	1.5	65.0	90	92.5 ± 0.8	92.2
13	3.0	1.0	50.0	90	87.0 ± 0.5	86.6
14	7.5	1.0	57.5	90	91.7 ± 0.4	91.6
15	7.5	1.5	50.0	90	90.0 ± 0.3	90.3
16	7.5	1.0	57.5	90	92.0 ± 0.4	91.6
17	3.0	1.0	65.0	90	86.5 ± 0.7	86.6
18	7.5	0.5	50.0	90	89.0 ± 0.7	89.0
19	7.5	1.0	57.5	90	91.2 ± 0.6	91.6
20	12	1.0	50.0	90	88.5 ± 0.5	88.6
21	12	1.0	65.0	90	89.5 ± 0.5	90.1
22	3.0	1.5	57.5	90	85.0 ± 0.8	85.2
23	7.5	1.0	57.5	90	91.2 ± 0.4	91.6
24	12	1.0	57.5	120	88.5 ± 0.2	88.3
25	7.5	0.5	57.5	120	88.5 ± 0.3	88.7
26	7.5	1.0	65.0	120	89.5 ± 0.3	89.7
27	3.0	1.0	57.5	120	84.7 ± 0.5	84.7
28	7.5	1.5	57.5	120	88.5 ± 0.7	88.4
29	7.5	1.0	50.0	120	89.6 ± 0.8	89.7

### 2.3. Artificial Intelligence Tools for Optimization

Statistical analysis was performed based on data collected according to the set of experimental matrices based on BBD. The adequacy of the model tested for statistical examination resulted in a better correlation coefficient with a value of 0.9899 (close to 1); therefore, model-derived empirical relationships (including all terms: linear, quadratic, and interaction) can be employed to locate the optimal transesterification parametric conditions for maximizing the biodiesel yield. The present work attempted to optimize the transesterification process using three heuristic search algorithms: BB-BC, FA, and GWO. Note that the performance of the algorithm (solution accuracy and computation time) varies depending on the domain of the problem [67–69]. The present work employed three state-of-the-art algorithms (FA, GWO, and BB-BC), whose performances have recently been examined with the aim of maximizing the yield.

#### 2.3.1. Firefly Algorithm

In 2010, Yang proposed the FA (family of swarm intelligence), which mimics the flashing patterns and behavior of fireflies [73]. FA was successfully applied to optimize various problems associated with distinguished applications (engineering, image processing, physics, robotics, economics, and so on) [74]. The flashing behavior and bioluminescent communication of fireflies use the following three rules and assumptions while determining solutions to optimization problems such as [74–76]:

1. Fireflies are unisex; regardless of sex, the fireflies attract each other.
2. A brighter firefly attracts partners with less brightness (regardless of gender), which ensures an efficient approach to determining the best partner. The attractiveness toward the brightest (intensity of agent or insect) firefly ensures the best or optimal solution, whereas attractiveness decreases when the distance between two fireflies increases, according to Equation (2).

$$I \propto \frac{1}{r^2} \tag{2}$$

3. Fireflies show random movement when the firefly brightness remains identical or equal.
4. If the light is traveling through a material with light absorption coefficient  $\gamma$ , the light intensity at  $r$  from the source may be given by Equation (3).

$$I = I_0 e^{-\gamma r^2} \tag{3}$$

5. The brightest firefly will conduct a local search by randomly traveling about its surroundings. As a result, if firefly  $j$  is brighter than firefly  $I$ , firefly  $I$  will travel towards firefly  $j$  using the updating formula in Equation (4).

$$x_i := x_i + \underbrace{\beta_0 e^{-\gamma r_{ij}^2}}_{=\beta} (x_j - x_i) + \alpha(\epsilon() - 0.5) \tag{4}$$

where  $\beta_0$  is the attractiveness of  $x_j$  at  $r = 0$ ;  $I_0$  is light intensity at the source;  $\gamma$  defines the extent to which the updating process is affected by the distance between the two fireflies,  $\alpha$  is an algorithm variable for the random movement step length, and  $\epsilon()$  is a uniform distribution random vector with values ranging from 0 to 1.

#### 2.3.2. Big-Bang Big-Crunch Algorithm

BB-BC is a novel gradient-free optimization algorithm based on a theory that suggests the universe possesses two phases—the big bang (BB) and the big crunch (BC)—proposed by Erol and Eksin in 2006 [77,78]. The BB-BC algorithm outperforms the evolutionary genetic algorithm; the algorithm converges to solutions at a higher speed and possesses a low computation time [77,79]. The fundamental characteristics of the BB phase ensure the

production of disorder and randomness by energy consumption; the particles that were randomly distributed in the BB phase are replaced with ones featuring better characteristics during the BC phase [80]. The steps involved in determining solutions to the optimization problems for the BB-BC algorithms are discussed below [69,77,80]:

1. The initial set of candidate solutions is distributed randomly according to the search space.
2. The fitness function values corresponding to individual candidate solutions are determined.
3. The center of mass based on the convergence operator is estimated, which has many inputs and generates a single output. The global fitness values are estimated according to the center of mass.
4. As iteration proceeds, the computation of new or best candidate solutions (i.e., fitness function values) is generated by the addition/subtraction of a random number around the center of mass.
5. The termination criterion has been tested for the pre-set goal. If the termination criterion has been met, the algorithm stops; otherwise, the above procedure will repeat.

### 2.3.3. Grey Wolf Optimization Algorithm

In 2014, S. Mirjalilli was credited for developing the GWO, which mimics the hunting mechanism and social hierarchy (alpha ( $\alpha$ ) at the top, followed by beta ( $\beta$ ), delta ( $\delta$ ), and omega ( $\omega$ )) of grey wolves [81]. Grey wolf are animals that prefer to live in packs or groups (5–12 individuals); each pack or group is categorized into four levels, one with respect to the other, in a social hierarchy [82]. Alpha wolves occupy the top position (referred to as a leader, which may be either male or female), whose main function is to make decisions for the pack regarding sleeping place, hunting, and wake-up time [83]. Note that  $\alpha$  wolves are strongest in a pack when the decisions made must be obeyed by the other individuals of the social hierarchy. Beta wolves help alpha wolves in making decisions (based on the orders of the alpha and then providing feedback) and are treated as potential candidates for substituting alpha wolves when they become old or die. Delta wolves dominate the omega and follow the orders of alpha and beta. Delta wolves serve as scouts (responsible for searching for boundaries and alerting the pack when they encounter dangerous situations), sentinels (ensuring security), elders (potential candidates for the next generation of alpha and beta), hunters (responsible for preparing food for the pack), and caretakers (caring for wolves in the pack that are sick, injured, or weak).

In GWO, grey wolves hunt for prey with the help of a pack (predefined number of grey wolves) in a multi-dimensional space at many spatial locations [84]. The fitness function values during optimization are computed based on the different positions of grey wolves and the distance of prey. As iteration progresses, the individual grey wolf adjusts its position towards a better position, and the best solutions are recorded during the course of action. Note that GWO mainly attempts to determine the shortest possible path that allows the grey wolves to reach their prey. The steps involved in locating the optimal solutions are performed by the following four steps [81,85]:

1. *Exploration*: each member switches positions with the others in order to follow, chase, and approach the victim or prey.
2. *Encircling*: grey wolf positions are updated based on the three best wolves (alpha, beta, and delta) in the search space around the prey.
3. *Hunting*: grey wolves possess greater ability and knowledge and determine the prey's location or position and encircle them. Alpha wolves lead the hunt, whereas delta and beta wolves join later. The positions of omega wolves are adjusted with reference to the top three fittest individuals of a population ( $\alpha$ ,  $\beta$ , and  $\delta$ ).
4. *Attacking the prey*: grey wolves terminate the hunting process only after ensuring the prey stops moving.

### 3. Results and Discussion

The results of the experimental input–output data, contributions of individual and interaction variables, curvature effect analysis, regression equations, and model statistical adequacies are discussed. The optimized set of transesterification conditions that maximize the biodiesel yield was determined and compared to the efficiency of three artificial intelligence tools (BB-BC, GWO, and FA). The physicochemical properties of NS-based biofuels are discussed.

#### 3.1. Experimental Input–Output Data Collection and Analysis

BBD-based experimental matrices are designed for four input variables (M:O, CC, Rt, and RT) and measure the output—biodiesel yield (see Table 3). Each experiment was repeated thrice, and average values corresponding to yield were recorded. It was observed from the total 29 transesterification experimental sets that the maximum and minimum deviation from the average biodiesel yield was found to be  $\pm 0.8$  and  $\pm 0.2$ , respectively (see Table 3).

#### 3.2. Main Effect Parameter Analysis

To identify the contributions of specific factors and perform statistical analysis, the Design-Expert software (version 11) was used. The effect of individual factors on the performance of biodiesel yield is explained below.

##### 3.2.1. Effect of Methanol-to-Oil Molar Ratio

Experiments were performed after varying the M:O ratio in ranges of 3:1 to 12:1; their impact on biodiesel yield is analyzed, as shown in Figure 3. An increase in the concentration of the M:O ratio tends to increase the biodiesel yield up to the mid-values and thereafter decreases. The desired maximum biodiesel yield was attained approximately nearer to the mid-values of the M:O ratio (see Figure 3). As the M:O ratio increases in the reaction process, biodiesel yield tends to increase up to the mid-values of their respective levels. At lower values of the M:O ratio, the time required to complete the transesterification reaction (KOH reacts with methanol to yield methoxide, which is treated as an actual reactant in the transesterification process, and water, which causes partial hydrolysis of acylglycerides or the methyl ester formed) will be very high with less usage of methanol. After crossing the mid-values of the M:O ratio, the excess quantity of methanol results in a decrease in biodiesel yield. This occurs due to the interference of excess methanol with alkyl ester and glycerol separation by increasing glycerol solubility. This results in the dilution of a portion of the glycerol remaining in the alkyl ester phase, which causes the loss of ester due to soap formation. In addition, the presence of glycerol in the solution shifts the equilibrium back to the left and results in a decreased biodiesel yield. A similar trend corresponding to the effect of methanol-to-oil molar ratio on yield was reported with the transesterification of *Musa acuminata* peduncle [41] and *Pithecellobium dulce* seed oil [35].

##### 3.2.2. Effect of Catalyst Concentration

Figure 3 explains the effect of KOH catalyst concentration (varied between 0.5 to 1.5 wt.%) on the performance of biodiesel yield. Yield showed an increasing trend with the increased concentration of KOH catalyst up to 1.1 to 1.2 wt.% and thereafter the trend decreased. Excess concentration of catalyst poses a difficulty in the separation of the aqueous layer during water washing of methyl ester and dissolves the methyl ester formed in it. This effect could be due to the increased saponification reaction resulting in the formation of soap, thus reducing the biodiesel yield. The biodiesel obtained with an excessive amount of catalyst is very viscous, unstable, and readily solidified and cannot be used as fuel in CI engines. Moreover, an inadequate concentration of KOH in the reaction resulted in decreased methyl ester conversion [38,51]. Figure 3 shows the impact of the methanol-to-oil molar ratio, which showed a dominant effect over that of the catalyst concentration.

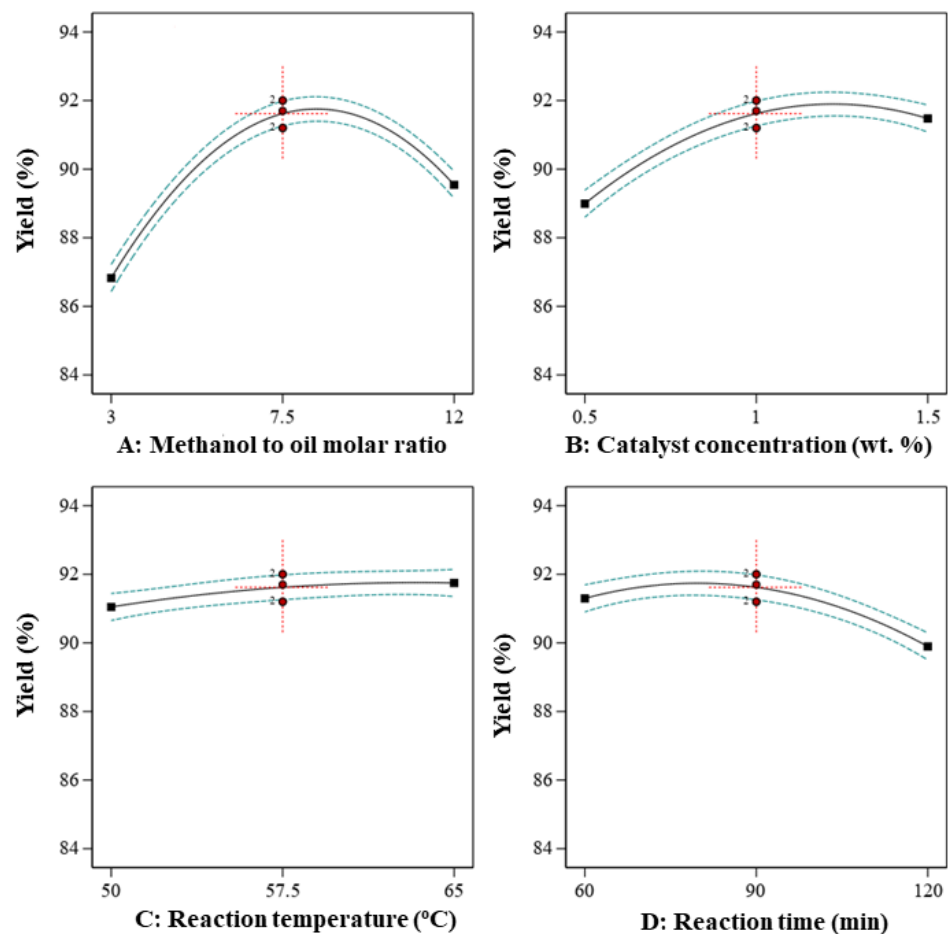


Figure 3. Main effect plot for biodiesel yield.

### 3.2.3. Effect of Reaction Temperature

The effect of reaction temperature during the transesterification process varied between the range of 50 to 65 °C. During transesterification at low reaction temperatures, the saponification reaction rate is higher and decreases with an increase in temperature. Higher reaction temperature increases or speeds up the reaction rates (because reactant molecules have higher energy, wherein reactions collide during transesterification), which favors the methanol-to-oil molar ratio to push the reaction that favors biodiesel yield. This could result in higher biodiesel yield when the reaction temperature is increased. It was observed that variations in reaction temperature resulted in a flat surface, which has a negligible effect on biodiesel yield. Similar observations are reported in the published literature [45].

### 3.2.4. Effect of Reaction Time

Figure 3 outlines the impact of reaction times ranging from 60 to 120 min on biodiesel output. Initially, the reaction of biodiesel yield was very fast after 60 min of reaction time, and therefore, the biodiesel yield increased. This occurs due to retention time for the reaction occurring up to 80 min in duration and then remaining relatively constant until 90 min; thereafter, the biodiesel yield started decreasing as the reaction time further increased. This occurred as the reaction reached equilibrium, and hence a reverse reaction started to occur. A longer reaction time decreases the biodiesel yield, which might be due to the increased probability of biodiesel hydrolysis under alkaline conditions [86,87]; therefore, it is of great importance to immediately separate the produced biodiesel from the reaction mixture once reaching the required reaction time. A higher reaction time decreases the biodiesel yield, which has negative effects, such as increased energy consumption and

reduced process efficiency [37]. Similar trends were observed with the transesterification process carried out for biodiesel conversion [38].

### 3.3. Surface Plot Analysis

We performed a three-dimensional surface plot analysis to examine the interaction factor (two factors varied simultaneously between their operating levels when the other factors stayed at fixed middle levels) effects on the performance of biodiesel yield.

1. Figure 4a explains the interaction factor effects of M:O and CC, where a reaction time of 90 min and a temperature of 57.5 °C were kept at fixed mid-values. A gradual reduction in biodiesel yield was observed after the mid-point values of both M:O and CC. The desired higher biodiesel yield was found to be nearer the mid-values of M:O and CC. Excess quantity of M:O results in an increase in the glycerol solubility, whereas a higher amount of CC results in higher viscosity, which then affects the mixing ability and produces soap formation and emulsions, which ensures lower biodiesel yield. Similar observations are reported for *Pithecellobium dulce* seed oil [35] and flaxseed oil [45].
2. The impact of two variables (such as M:O and RT) varied between their respective levels after the two parameters were held at respective mid-values (see Figure 4b). A simultaneous increase in M:O and RT, wherein the rate of reaction increases such that it pushes the reaction forward, could favor biodiesel yield. When compared to M:O, the impact of reaction temperature was found to be negligibly small. A similar effect was obtained corresponding to the transesterification of soyabean oil with ethanol [38].
3. Figure 4c displays the interaction factor effects of M:O and Rt when two of the parameters (i.e., reaction temperature of 57.5 °C and catalyst concentration of 7.5 wt.%) are maintained constant. The biodiesel yield tends to increase with increased values of M:O and tends to decrease with an increase in reaction time. Higher biodiesel yield was obtained at a shortened duration corresponding to the middle level of the reaction temperature and catalyst concentration.
4. The effect of CC and RT was analyzed after varying two factors simultaneously between their operating levels (refer to Figure 4d). The biodiesel yield tends to increase with increased values of catalyst concentration up to 1 wt.%, wherein the reaction temperature was found to have negligible impact. It was also observed that yield was found to decrease with high values of catalyst concentration and reaction temperatures that favor the triglyceride saponification reaction. The results are analogous to biodiesel yield production from *Jatropha* seed oil [88].
5. The impact on biodiesel yield by varying two variables simultaneously, such as CC and Rt (refer to Figure 4e). The combination of higher catalyst concentration and mid-values of reaction time resulted in higher biodiesel yield. An increase in weight percent of catalyst concentration ensures supplying more catalyst for the reacting samples that could accelerate the biodiesel yield. It was also observed that there was no significant improvement in the yield after ensuring a sufficient reaction time of 90 min.
6. The effect of reaction time and reaction temperature when variables simultaneously varied between the operating levels were analyzed for the fixed values of CC of 1 wt.% and M:O of 7.5 (see Figure 4f). The resultant surface plot is seen to appear almost flat, which clearly indicates the biodiesel yield tends to have negligible influence on the interaction effect of reaction temperature and time. With increased values of reaction time, the biodiesel yield was found to have a negligible effect with an increasing trend (required time to attain the equilibrium point of a reaction wherein reaction rate increases), and beyond the limit, there might be a possibility to attain a reversible reaction when the reaction rate increases with the increased temperature [89].

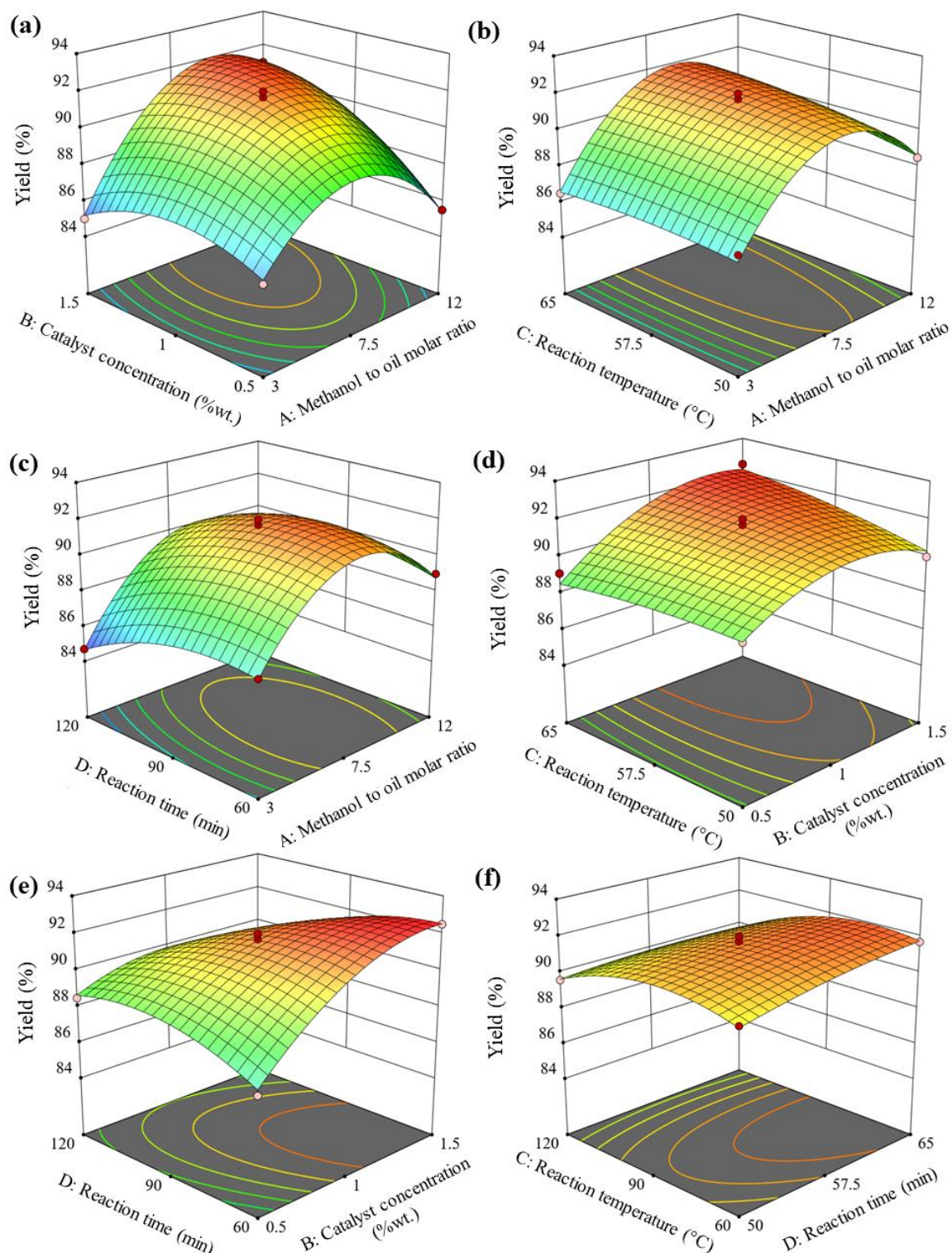


**Figure 4.** The 3D surface plots of transesterification variables vs. biodiesel yield: (a) M:O and CC, (b) M:O and RT, (c) M:O and Rt, (d) CC and RT, (e) CC and Rt, and (f) Rt and RT.

### 3.4. Regression Model for Biodiesel Yield

The BBD model was used that could correlate independent variables (M:O, CC, Rt, and RT) and dependent variables (biodiesel yield) based on experiments performed. The experimental input–output data that could fit models without any bias is presented in Table 4.

**Table 4.** Fitted models correspond to experimental input–output data.

Model	Regression Equation	Regression Coefficient
Linear	Yield = 83.78 + 0.302 A + 2.483 B + 0.047 C – 0.027 D	R <sup>2</sup> = 0.3141, and Adj. R <sup>2</sup> = 0.1998
Linear + Interaction	Yield = 89.297 – 1.304 A – 3.467 B – 0.067 C + 0.1264 D + 0.667 AB + 0.011 AC + 0.0033AD + 0.16 BC – 0.0917 BD – 0.0014 CD	R <sup>2</sup> = 0.4437, and Adj. R <sup>2</sup> = 0.1347
Linear + Interaction + Square	Yield = 54.44389 + 1.24074 A + 7.61333 B + 0.388222 C + 0.330889 D + 0.666667 AB + 0.011111 AC + 0.003333 AD + 0.16 BC – 0.0916670 BD – 0.001444 CD – 0.16963 A <sup>2</sup> 5.54 B <sup>2</sup> – 0.003956 C <sup>2</sup> – 0.001136 D <sup>2</sup>	R <sup>2</sup> = 0.9869, and Adj. R <sup>2</sup> = 0.9737

The model’s statistical adequacy was evaluated based on regression coefficients. Note that the model with full quadratic terms (linear + interaction + square) resulted in a better regressor coefficient equal to 0.9869 (close to 1), which clearly indicates the best fit model. The adjusted R<sup>2</sup> (excluding insignificant terms: AC, CD, and C<sup>2</sup> from the model) value was found equal to 0.9737. The best fit quadratic model represents biodiesel yield as a mathematical function of transesterification variables (M:O, CC, Rt, and RT).

$$\begin{aligned}
 \text{Yield (\%)} = & +54.44389 + 1.24074 A + 7.61333 B + 0.388222 C + 0.330889 D \\
 & +0.666667 AB + 0.011111 AC + 0.003333 AD + 0.16 BC - 0.0916670 BD \\
 & - 0.001444 CD - 0.16963 A^2 - 5.54 B^2 - 0.003956 C^2 - 0.001136 D^2
 \end{aligned}
 \tag{5}$$

The experimental data were analyzed for the developed quadratic model that could estimate linear, square, and interaction factor effects. All linear terms (M:O, CC, RT, and Rt) were found to have significant contributions (as their *p*-values < 0.05). The effect of the reaction temperature was found to be significant as their effect (measured with F-value) was found to be comparatively lower than M:O, CC, and Rt. This can be clearly seen in the main effect plot result shown in Figure 3. The square terms of M:O, CC, and Rt were found to be significant as their *p*-values are <0.05, which clearly indicates their relationship with biodiesel yield is non-linear. The squared term of reaction temperature was found to be insignificant (*p*-value > 0.05), and hence the relationship with biodiesel yield was found to be linear. The curvature effects are in good agreement with statistical *p*-values of squared terms of transesterification variables (see Table 5). Although all individual terms were found to be significant, the interaction terms (M:O and RT, and RT and Rt) were found to be insignificant with negligible influence on biodiesel yield. Excluding insignificant terms (M:O × RT, RT × Rt, and RT<sup>2</sup>) from the model-derived regression equation creates imprecise input–output relationships and reduces the prediction accuracy; therefore, the model was tested for prediction accuracy with experimental values with inclusion of all terms in the equation resulted in the best fit data, close to the trend line (see Figure 5). The better prediction ensures the regression equations derived for predicting the biodiesel yield are accurate and can be used to perform optimization.

**Table 5.** Analysis of variance for biodiesel yield.

Source	Sum of Squares	DF	Mean Square	F-Value	<i>p</i> -Value
Model	150.77	14	10.77	75.62	0.0001
M:O	22.14	1	22.14	155.47	0.0001
CC	18.50	1	18.50	129.91	0.0001
RT	1.47	1	1.47	10.32	0.0063
Rt	5.88	1	5.88	41.29	0.0001
M:O × CC	9.00	1	9.00	63.19	0.0001
M:O × RT	0.5625	1	0.5625	3.95	0.0668

Table 5. Cont.

Source	Sum of Squares	DF	Mean Square	F-Value	<i>p</i> -Value
M:O × Rt	0.8100	1	0.8100	5.69	0.0318
CC × RT	1.44	1	1.44	10.11	0.0067
CC × Rt	7.56	1	7.56	53.10	0.0001
RT × Rt	0.4225	1	0.4225	2.97	0.1070
M:O <sup>2</sup>	76.54	1	76.54	537.41	0.0001
CC <sup>2</sup>	12.44	1	12.44	87.37	0.0001
RT <sup>2</sup>	0.3211	1	0.3211	2.25	0.1554
Rt <sup>2</sup>	6.78	1	6.78	47.62	0.0001
Residual	1.99	14	0.1424		
Lack of Fit	1.35	10	0.1346	0.8308	0.6322
Pure Error	0.6480	4	0.1620		
Cor Total	152.77	28			

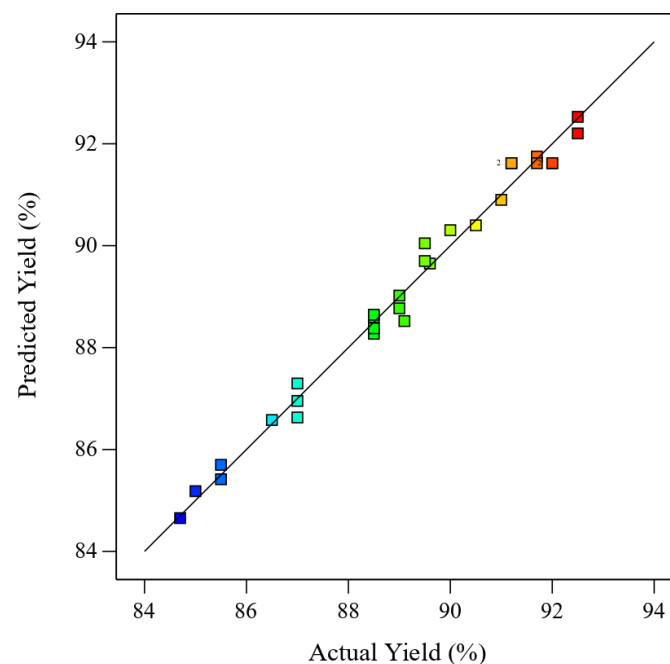


Figure 5. Predicted versus actual biodiesel yield.

### 3.5. Summary Results of Optimization Algorithms

The set of optimal transesterification conditions that maximize the biodiesel yield was predicted by applying three algorithms (BB-BC, GWO, and FA). Equation (5) serves as an objective function to conduct optimization for maximum biodiesel yield. The algorithm search with the upper and lower bounds of transesterification variables was used for experimentation (see Table 2). The efficacy of all three algorithms was evaluated on the basis of computation time and solution accuracy. Note that the common algorithm parameters, such as population size and iterations to terminate the program, are kept fixed to 100 and 1000, respectively. The results attained from each algorithm were tested 10 times, and the best solution corresponds to the fitness value and computation time is recorded (see Table 6). Tuning algorithm-specific parameters (GWO: convergence constant, FA: randomness, absorption coefficient, randomness reduction; BB-BC: exploration factor) is of the utmost importance, as it could determine the optimization efficiency [78,90,91]. Tuning algorithm-specific parameters was carried out to maximize the fitness values (biodiesel yield (%)) and the optimal parameters were selected after the algorithm ran for successive trials. The optimal transesterification conditions were thus determined after fixing algorithm-specific parameters and common parameters (population size: 100 and iterations: 1000) that could result in maximum biodiesel yield. The fitness value (i.e., maximum yield)

corresponding to all three algorithms (GWO, FA, and BB-BC) was found to be equal to 94.15%, 94.15%, and 93.07%, respectively. Note that GWO and FA resulted in identical optimal conditions, as opposed to that obtained for BB-BC. GWO uses a constant convergence parameter (wherein the search radius of grey wolves makes a better trade-off between exploration and exploitation), which ensures better results. Confirmation experiments were conducted corresponding to the optimal transesterification conditions (M:O: 9.32, CC: 1.5 wt.%, RT: 65 °C, and Rt: 60 s), resulting in experimental values of biodiesel yield equal to 95.3% ± 0.5%. Table 1 details the biodiesel yield conversion that corresponds to various feedstocks [35,37,40,42,43,47,51,53,55], which is comparatively less than that of NS-based biodiesel yield equal to 95.3% ± 0.5%; however, NS-based biodiesel yield was comparatively less than other feedstocks [41,44,45,47,48,50,52,54,56]. The difference in biodiesel yield for various feedstocks is dependent primarily on the FFA of the feed stocks used, which in turn affects the cost [92]. The presence of higher FFA (>2%) in oil resulted in decreased biodiesel yield and it varied with the type of feedstocks used for biodiesel production [93,94]. The niger seed oil possesses 7% FFA, and hence acid-catalyzed esterification was adopted before the actual transesterification process. Note that the increase in the number of steps in producing biodiesel resulted in a decrease in biodiesel yield. Similar outcomes have been reported by other researchers [95,96]. The MATLAB software platform was used on a PC (RAM: 4 GB, Processor: Intel Core i3 @ 1.2 GHz CPU) to perform a computation of biodiesel yield. The computation time corresponding to the maximum fitness values were recorded and are found to be equal to 0.8 s for BB-BC, 15.06 s for FA, and 1.66 s for GWO, respectively. BB-BC showed lesser computation time than GWO and FA, which might be due to tuning only one algorithm-specific parameter and better exploration capability and search mechanisms; however, GWO is recommended to obtain the maximum biodiesel yield with a better convergence rate of 1.66 s.

**Table 6.** Optimization of transesterification parameters using three algorithms.

Algorithms	Algorithm Specific Parameters	Fitness Value (Yield%)	Computation Time (seconds)	Transesterification Condition
GWO	Convergence constant = 0.5	94.15%	1.66	M:O = 9.32; CC = 1.5 wt.%; RT = 65 °C; Rt = 60 s
FA	Randomness, $\alpha = 0.9$ ; Absorption coefficient, $\gamma = 1$ ; Randomness reduction, $\beta = 0.6$	94.15%	15.06	M:O = 9.32; CC = 1.5 wt.%; RT = 65 °C; Rt = 60 s
BB-BC	Exploration factor = 14	93.07%	0.8	M:O = 9.02; CC = 1.47 wt.%; RT = 63.8 °C; Rt = 86.1 s

### 3.6. Physicochemical Properties Evaluation of Biodiesel Yield and NS Oil

Evaluation of physicochemical properties is essential to examine the practicality of fuels (niger seed oil, NS-oil-derived biodiesel yield) to use in diesel engines as per ASTM D6751-15C. The average of three values corresponding to each property was recorded to conduct the analysis [45]. Specific gravity is one of the paramount physicochemical properties that could influence the fuel injection system of a combustion engine. The specific gravity of NS oil is reduced from 0.93 to 0.88 (after biodiesel conversion viz. transesterification process). Transesterification of biodiesel yield resulted in a specific gravity within the acceptable ranges (0.87 to 0.89) as per biodiesel standard. Viscosity corresponds to fuel samples (NS oil, NS-oil-derived biodiesel yield) that affect the diesel engine fuel injection system. The higher viscosity of (7.4 mm<sup>2</sup>/s) NS oil could result in incomplete combustion due to poor atomization and the deposit of carbon on the injector. After transesterification of NS oil, the kinematic viscosity of biodiesel yield was found to be reduced to 3.9 mm<sup>2</sup>/s (falling under the permissible standard limit: 1.9 to 6.0). The calorific value is of paramount importance that defines the energy content in the samples. The determined calorific values for NS oil and biodiesel yield were found to be equal to 38,560 kJ/kg and 40,400 kJ/kg, respectively. The 35,000 kJ/kg is the minimum standard calorific value to be tested in a diesel engine. The acid value of NS oil reduces from

14 mg KOH/g to 0.36 mg KOH/g. The acid value obtained for biodiesel yield resulted in acceptable test limits for biodiesel equal to 0.5 mg KOH/g. The copper strip corrosion, cloud point, pour point, flash point, iodine value, and cetane number are found to be equal to 1, 14 °C, 9 °C, 0.01% *w/w*, and 65.50, respectively, and are within the permissible limit corresponding to the biodiesel standard.

#### 4. Conclusions

This work presents a cost-effective approach to biodiesel conversion using feed stock selection, the transesterification process, experiments, process parameters, prediction, and optimization. The following conclusions are drawn:

1. NS grown in hilly areas with less fertile soil, including the byproducts of seeds, has potential medicinal value. Niger seeds possess higher oil content (37–50%) and are therefore treated as cost-effective feedstock.
2. Transesterification parameters (M:O, Rt, CC, and RT) were studied experimentally at reduced trials using BBD. The effect of all factors (linear + square + interaction) on the performance of biodiesel yield was studied. Among linear terms: M:O was the most contributing factor, followed by CC, Rt, and RT. The square terms of M:O, CC, and Rt were found to be significant, and thus, the relationship with biodiesel yield was found to be non-linear, whereas reaction temperature has a linear relationship with biodiesel yield. Two interaction terms (M:O × RT, RT × Rt) were found to be insignificant for biodiesel yield, whereas M:O with CC interaction term showed a dominant effect followed by CC with Rt, CC with RT, M:O with Rt, M:O with RT, respectively.
3. The BBD-model-derived empirical equation predicted the biodiesel yield with the best fit and showed a good regression coefficient for the full quadratic model (terms: linear + square + interaction) found equal to 0.9869. The adjusted  $R^2$  (excluding insignificant terms: M:O × RT, RT × Rt, and  $RT^2$  from the model) value was found to be equal to 0.9737; therefore, model equations are statistically significant for conducting predictions (without performing the actual experiments) and optimization.
4. Three artificial intelligence algorithms (BB-BC, GWO, FA) were applied to conduct optimization that could maximize the biodiesel yield. Transesterification parameters (M:O, Rt, CC, and RT) were optimized, and the resulting maximum fitness value (biodiesel yield) was found to be equal to 94.15% for both BB-BC and GWO, respectively, and 93.07% for FA. The confirmation experiments performed for optimized transesterification conditions (M:O = 9.32; CC = 1.5 wt.%; RT = 65 °C; Rt = 60 s) resulted in a biodiesel yield equal to  $95.3 \pm 0.5\%$ .
5. All three algorithms were tested for computational efficiency, and the results showed 0.8 s for BB-BC, 1.66 s for GWO, and 15.06 s for FA. Although BB-BC is computationally competent, it needs to compromise for solution accuracy; therefore, GWO is recommended to obtain a better solution accuracy and computation time.
6. The physicochemical properties of biodiesel fuel were tested according to the ASTM standards; results were in good agreement (the kinematic viscosity, acid value, calorific value, copper strip corrosion, cloud point, pour point, flash point, sulfur content, and cetane number were found to be equal to 3.9 mm<sup>2</sup>/s, 0.36 mg KOH/g, 40,400 kJ/kg, 1, 14 °C, 9 °C, 0.01% *w/w*, and 65.50) and were within the permissible limit corresponding to the biodiesel standard to use in diesel engines.

**Author Contributions:** Conceptualization, S.H.V., A.L., K.S., M.P.G.C., C.P.S., and M.B.D.; methodology, S.H.V., A.L., C.P.S., and M.P.G.C.; software, M.P.G.C. and A.R.; validation, P.B.A., E.L., K.S., and A.R.; formal analysis, E.L., A.R., P.B.A., and K.S.; investigation, S.H.V., A.L., K.S., M.P.G.C., C.P.S., and M.B.D.; resources, M.B.D., C.P.S., and M.P.G.C.; writing—original draft preparation, M.P.G.C., K.S., E.L., and A.R.; writing—review and editing, S.H.V., A.L., C.P.S., M.B.D., and P.B.A. All authors have read and agreed to the published version of the manuscript.

**Funding:** This research received no external funding.

**Institutional Review Board Statement:** Not applicable.

**Informed Consent Statement:** Not applicable.

**Data Availability Statement:** Not applicable.

**Conflicts of Interest:** The authors declare no conflict of interest.

## Nomenclature

A	Methanol-to-oil molar ratio
ASTM	American Society for Testing and Materials
B	Catalyst concentration
BBD	Box–Behnken design
BB-BC	Big-Bang Big-Crunch Algorithm
C	Reaction temperature
CC	Catalyst concentration
CCD	Central composite design
CCRD	Central composite rotatable design
D	Reaction time
FA	Firefly algorithm
GWO	Grey wolf optimization
MRAO	Methanol ratio of alcohol to oil
NaOH	Sodium hydroxide
NS	Niger seed
OMMR	Oil-to-methanol molar ratio
OMVR	Oil-to-methanol volume ratio
M: O	Methanol-to-oil molar ratio
NS	Niger seed
Rt	Reaction time
RT	Reaction temperature
RSM	Response surface methodology
$\alpha$	Randomness
$\gamma$	Absorption coefficient
$\beta$	Randomness reduction
R <sup>2</sup>	Regressor coefficient

## References

- Zakari, A.; Khan, I. Boosting economic growth through energy in Africa: The role of Chinese investment and institutional quality. *J. Chin. Econ. Bus. Stud.* **2022**, *20*, 1–21. [[CrossRef](#)]
- Muhammad, B.; Khan, M.K.; Khan, M.I.; Khan, S. Impact of foreign direct investment, natural resources, renewable energy consumption, and economic growth on environmental degradation: Evidence from BRICS, developing, developed and global countries. *Environ. Sci. Pollut. Res.* **2021**, *28*, 21789–21798. [[CrossRef](#)] [[PubMed](#)]
- Oyedepo, S.O. Energy and sustainable development in Nigeria: The way forward. *Energy Sustain. Soc.* **2012**, *2*, 15. [[CrossRef](#)]
- Olatomiwa, L.; Blanchard, R.; Mekhilef, S.; Akinyele, D. Hybrid renewable energy supply for rural healthcare facilities: An approach to quality healthcare delivery. *Sustain. Energy Technol. Assess.* **2018**, *30*, 121–138. [[CrossRef](#)]
- Banerjee, R.; Mishra, V.; Maruta, A.A. Energy poverty, health and education outcomes: Evidence from the developing world. *Energy Econ.* **2021**, *101*, 105447. [[CrossRef](#)]
- Sahoo, R.; Mondal, S.; Pal, S.C.; Mukherjee, D.; Das, M.C. Covalent–Organic Frameworks (COFs) as Proton Conductors. *Adv. Energy Mater.* **2021**, *11*, 2102300. [[CrossRef](#)]
- Tang, B.J.; Guo, Y.Y.; Yu, B.; Harvey, L.D. Pathways for decarbonizing China’s building sector under global warming thresholds. *Appl. Energy* **2021**, *298*, 117213. [[CrossRef](#)]
- Ntaribi, T.; Paul, D.I. The economic feasibility of Jatropha cultivation for biodiesel production in Rwanda: A case study of Kirehe district. *Energy Sustain. Dev.* **2019**, *50*, 27–37. [[CrossRef](#)]
- Thakur, A.K.; Kaviti, A.K.; Singh, R.; Gehlot, A. An overview of butanol as compression ignition engine fuel. *Int. J. Energy Clean Environ.* **2020**, *21*, 333–354. [[CrossRef](#)]
- Sarkar, A.; Sahu, D.; Das, D.; Behera, S.P.; Nayak, S.K.; Mandal, B.K. Effects of Ethanol as the Renewable fuel Blended with Gasoline on the Performance and Emission Characteristics of a Small Variable Compression Ratio Spark-Ignition Engine. *Int. J. Energy Clean Environ.* **2022**, *23*, 1–12. [[CrossRef](#)]
- Ahorsu, R.; Medina, F.; Constantí, M. Significance and challenges of biomass as a suitable feedstock for bioenergy and biochemical production: A review. *Energies* **2018**, *11*, 3366. [[CrossRef](#)]

12. Miraculas, G.A.; Bose, N.; Raj, R.E. Process parameter optimization for biodiesel production from mixed feedstock using empirical model. *Sustain. Energy Technol. Assess.* **2018**, *28*, 54–59. [[CrossRef](#)]
13. Ayoob, A.K.; Fadhil, A.B. Valorization of waste tires in the synthesis of an effective carbon based catalyst for biodiesel production from a mixture of non-edible oils. *Fuel* **2020**, *264*, 116754. [[CrossRef](#)]
14. Nascimento, L.; Ribeiro, A.; Ferreira, A.; Valério, N.; Pinheiro, V.; Araújo, J.; Vilarinho, C.; Carvalho, J. Turning Waste Cooking Oils into Biofuels—Valorization Technologies: A Review. *Energies* **2021**, *15*, 116. [[CrossRef](#)]
15. Toldrá-Reig, F.; Mora, L.; Toldrá, F. Developments in the use of lipase transesterification for biodiesel production from animal fat waste. *Appl. Sci.* **2020**, *10*, 5085. [[CrossRef](#)]
16. Binczarski, M.J.; Malinowska, J.Z.; Berłowska, J.; Cieciora-Wloch, W.; Borowski, S.; Cieslak, M.; Cieslak, M.; Puchowicz, D.; Witonska, I.A. Concept for the Use of Cotton Waste Hydrolysates in Fermentation Media for Biofuel Production. *Energies* **2022**, *15*, 2856. [[CrossRef](#)]
17. Pasawan, M.; Chen, S.S.; Das, B.; Chang, H.M.; Chang, C.T.; Nguyen, T.X.Q.; Qu, H.M.; Chen, Y.F. Ultrasonication Assisted Catalytic Transesterification of Ceiba Pentandra (Kapok) Oil Derived Biodiesel Using Immobilized Iron Nanoparticles. *Fuels* **2022**, *3*, 113–131. [[CrossRef](#)]
18. Maheswari, P.; Haider, M.B.; Yusuf, M.; Klemeš, J.J.; Bokhari, A.; Beg, M.; Othman, A.A.; Kumar, R.; Jaiswal, A.K. A review on latest trends in cleaner biodiesel production: Role of feedstock, production methods, and catalysts. *J. Clean. Prod.* **2022**, *355*, 131588. [[CrossRef](#)]
19. Salaheldeen, M.; Mariod, A.A.; Aroua, M.K.; Rahman, S.M.; Soudagar, M.E.M.; Fattah, I.M. Current state and perspectives on transesterification of triglycerides for biodiesel production. *Catalysts* **2021**, *11*, 1121. [[CrossRef](#)]
20. Ge, J.C.; Yoon, S.K.; Song, J.H. Comparative Evaluation on Combustion and Emission Characteristics of a Diesel Engine Fueled with Crude Palm Oil Blends. *Appl. Sci.* **2021**, *11*, 11502. [[CrossRef](#)]
21. Udayakumar, M.; Sivaganesan, S.; Sivamani, S. Process optimization of KOH catalyzed biodiesel production from crude sunflower-mahua oil. *Biofuels* **2022**, 1–9. [[CrossRef](#)]
22. Saravanan, A.; Murugan, M.; Reddy, M.S.; Parida, S. Performance and emission characteristics of variable compression ratio CI engine fueled with dual biodiesel blends of Rapeseed and Mahua. *Fuel* **2020**, *263*, 116751. [[CrossRef](#)]
23. Soudagar, M.E.M.; Khan, H.M.; Khan, T.M.; Razzaq, L.; Asif, T.; Mujtaba, M.A.; Hussain, A.; Farooq, M.; Ahmed, W.; Shahapurkar, K.; et al. Experimental analysis of engine performance and exhaust pollutant on a single-cylinder diesel engine operated using moringa oleifera biodiesel. *Appl. Sci.* **2021**, *11*, 7071. [[CrossRef](#)]
24. Wategave, S.P.; Banapurmath, N.R.; Sawant, M.S.; Soudagar, M.E.M.; Mujtaba, M.A.; Afzal, A.; Basha, J.S.; Alazwari, M.A.; Safaei, M.R.; Elfasakhany, A.; et al. Clean combustion and emissions strategy using reactivity controlled compression ignition (RCCI) mode engine powered with CNG-Karanja biodiesel. *J. Taiwan Inst. Chem. Eng.* **2021**, *124*, 116–131. [[CrossRef](#)]
25. Ajith, B.S.; Math, M.C.; Patel, G.C.M.; Parappagoudar, M.B. Analysis and optimisation of transesterification parameters for high-yield Garcinia Gummi-Gutta biodiesel using RSM and TLBO. *Aust. J. Mech. Eng.* **2020**, 1–16. [[CrossRef](#)]
26. Jaikumar, S.; Bhatti, S.K.; Srinivas, V. Experimental investigations on performance, combustion, and emission characteristics of Niger (*Guizotia abyssinica*) seed oil methyl ester blends with diesel at different compression ratios. *Arab. J. Sci. Eng.* **2019**, *44*, 5263–5273. [[CrossRef](#)]
27. Srikanth, H.V.; Godiganur, S.; Manne, B.; Bharath Kumar, S.; Spurthy, S. Niger seed oil biodiesel as an emulsifier in diesel–ethanol blends for compression ignition engine. *Int. J. Ambient. Energy* **2020**, 1–11. [[CrossRef](#)]
28. Quequeto, W.D.; Siqueira, V.C.; Nazario, C.E.D.; Junqueira, M.H.; Schoeningher, V.; Martins, E.A.S. Oil composition and physiological quality of Niger seeds after drying. *Acta Sci. Agron.* **2020**, *42*, e44398. [[CrossRef](#)]
29. Deme, T.; Haki, G.D.; Retta, N.; Woldegiorgis, A.; Geleta, M. Mineral and Anti-Nutritional Contents of Niger Seed (*Guizotia abyssinica* (Lf) Cass., Linseed (*Linum usitatissimum* L.) and Sesame (*Sesamum indicum* L.) Varieties Grown in Ethiopia. *Foods* **2017**, *6*, 27. [[CrossRef](#)]
30. Mohseni, N.M.; Mirzaei, H.; Moghimi, M. Optimized extraction and quality evaluation of Niger seed oil via microwave-pulsed electric field pretreatments. *Food Sci. Nutr.* **2020**, *8*, 1383–1393. [[CrossRef](#)]
31. Melaku, E.T. Evaluation of Ethiopian Nigerseed (*Guizotia abyssinica* Cass) Production, Seed Storage and Virgin Oil Expression. Ph.D. Thesis, Humboldt Universität zu Berlin, Berlin, Germany, 2013; 187p.
32. Shadangi, K.P.; Mohanty, K. Production and characterization of pyrolytic oil by catalytic pyrolysis of Niger seed. *Fuel* **2014**, *126*, 109–115. [[CrossRef](#)]
33. Pradhan, K.; Mishra, R.; Paikary, R. Genetic variability and character association in niger. *Indian J. Genet. Plant Breed.* **1995**, *44*, 457–459.
34. Alemaw, G.; Wold, A.T. An agronomic and seed-quality evaluation of noug (*Guizotia abyssinica* Cass.) germplasm in Ethiopia. *Plant Breed.* **1995**, *114*, 375–376. [[CrossRef](#)]
35. Sekhar, S.C.; Karuppasamy, K.; Vedaraman, N.; Kabeel, A.E.; Sathyamurthy, R.; Elkelawy, M.; Bastawissi, H.A.E. Biodiesel production process optimization from *Pithecellobium dulce* seed oil: Performance, combustion, and emission analysis on compression ignition engine fuelled with diesel/biodiesel blends. *Energy Convers. Manag.* **2018**, *161*, 141–154. [[CrossRef](#)]
36. Thoai, D.N.; Tongurai, C.; Prasertsit, K.; Kumar, A. Review on biodiesel production by two-step catalytic conversion. *Biocatal. Agric. Biotechnol.* **2019**, *18*, 101023. [[CrossRef](#)]

37. Supraja, K.V.; Behera, B.; Paramasivan, B. Optimization of process variables on two-step microwave-assisted transesterification of waste cooking oil. *Environ. Sci. Pollut. Res.* **2020**, *27*, 27244–27255. [[CrossRef](#)]
38. Silva, G.F.; Camargo, F.L.; Ferreira, A.L. Application of response surface methodology for optimization of biodiesel production by transesterification of soybean oil with ethanol. *Fuel Process. Technol.* **2011**, *92*, 407–413. [[CrossRef](#)]
39. Parappagoudar, M.B.; Pratihari, D.K.; Datta, G.L. Linear and non-linear statistical modelling of green sand mould system. *Int. J. Cast Met. Res.* **2007**, *20*, 1–13. [[CrossRef](#)]
40. Onoji, S.E.; Iyuke, S.E.; Igbafe, A.I.; Daramola, M.O. Transesterification of rubber seed oil to biodiesel over a calcined waste rubber seed shell catalyst: Modeling and optimization of process variables. *Energy Fuels* **2017**, *31*, 6109–6119. [[CrossRef](#)]
41. Balajii, M.; Niju, S. A novel biobased heterogeneous catalyst derived from *Musa acuminata* peduncle for biodiesel production—Process optimization using central composite design. *Energy Convers. Manag.* **2019**, *189*, 118–131. [[CrossRef](#)]
42. Rokni, K.; Mostafaei, M.; Soufi, M.D.; Kahrizi, D. Microwave-assisted intensification of transesterification reaction for biodiesel production from camelina oil: Optimization by Box-Behnken Design. *Bioresour. Technol. Rep.* **2022**, *17*, 100928. [[CrossRef](#)]
43. Vahid, B.R.; Saghatoleslami, N.; Nayebzadeh, H.; Toghiani, J. Effect of alumina loading on the properties and activity of SO<sub>4</sub><sup>2-</sup>/ZrO<sub>2</sub> for biodiesel production: Process optimization via response surface methodology. *J. Taiwan Inst. Chem. Eng.* **2018**, *83*, 115–123. [[CrossRef](#)]
44. Mares, E.K.L.; Gonçalves, M.A.; da Luz, P.T.S.; da Rocha Filho, G.N.; Zamian, J.R.; da Conceição, L.R.V. Acai seed ash as a novel basic heterogeneous catalyst for biodiesel synthesis: Optimization of the biodiesel production process. *Fuel* **2021**, *299*, 120887. [[CrossRef](#)]
45. Ahmad, T.; Danish, M.; Kale, P.; Geremew, B.; Adeboju, S.B.; Nizami, M.; Ayoub, M. Optimization of process variables for biodiesel production by transesterification of flaxseed oil and produced biodiesel characterizations. *Renew. Energy* **2019**, *139*, 1272–1280. [[CrossRef](#)]
46. Qu, T.; Niu, S.; Zhang, X.; Han, K.; Lu, C. Preparation of calcium modified Zn-Ce/Al<sub>2</sub>O<sub>3</sub> heterogeneous catalyst for biodiesel production through transesterification of palm oil with methanol optimized by response surface methodology. *Fuel* **2021**, *284*, 118986. [[CrossRef](#)]
47. Sharma, A.; Kodgire, P.; Kachhwaha, S.S. Biodiesel production from waste cotton-seed cooking oil using microwave-assisted transesterification: Optimization and kinetic modeling. *Renew. Sustain. Energy Rev.* **2019**, *116*, 109394. [[CrossRef](#)]
48. Sharma, A.; Kodgire, P.; Kachhwaha, S.S. Investigation of ultrasound-assisted KOH and CaO catalyzed transesterification for biodiesel production from waste cotton-seed cooking oil: Process optimization and conversion rate evaluation. *J. Clean. Prod.* **2020**, *259*, 120982. [[CrossRef](#)]
49. Yesilyurt, M.K.; Arslan, M.; Eryilmaz, T. Application of response surface methodology for the optimization of biodiesel production from yellow mustard (*Sinapis alba* L.) seed oil. *Int. J. Green Energy* **2019**, *16*, 60–71. [[CrossRef](#)]
50. Milano, J.; Ong, H.C.; Masjuki, H.H.; Silitonga, A.S.; Chen, W.H.; Kusumo, F.; Dharma, S.; Sebayang, A.H. Optimization of biodiesel production by microwave irradiation-assisted transesterification for waste cooking oil-*Calophyllum inophyllum* oil via response surface methodology. *Energy Convers. Manag.* **2018**, *158*, 400–415. [[CrossRef](#)]
51. Elango, R.K.; Sathiasivan, K.; Muthukumaran, C.; Thangavelu, V.; Rajesh, M.; Tamilarasan, K. Transesterification of castor oil for biodiesel production: Process optimization and characterization. *Microchem. J.* **2019**, *145*, 1162–1168. [[CrossRef](#)]
52. Pooja, S.; Anbarasan, B.; Ponnusami, V.; Arumugam, A. Efficient production and optimization of biodiesel from kapok (*Ceiba pentandra*) oil by lipase transesterification process: Addressing positive environmental impact. *Renew. Energy* **2021**, *165*, 619–631. [[CrossRef](#)]
53. Dehghan, L.; Golmakani, M.T.; Hosseini, S.M.H. Optimization of microwave-assisted accelerated transesterification of inedible olive oil for biodiesel production. *Renew. Energy* **2019**, *138*, 915–922. [[CrossRef](#)]
54. Pascoal, C.V.P.; Oliveira, A.L.L.; Figueiredo, D.D.; Assunção, J.C.C. Optimization and kinetic study of ultrasonic-mediated in situ transesterification for biodiesel production from the almonds of *Syagrus cearensis*. *Renew. Energy* **2020**, *147*, 1815–1824. [[CrossRef](#)]
55. Vishal, D.; Dubey, S.; Goyal, R.; Dwivedi, G.; Baredar, P.; Chhabra, M. Optimization of alkali-catalyzed transesterification of rubber oil for biodiesel production & its impact on engine performance. *Renew. Energy* **2020**, *158*, 167–180. [[CrossRef](#)]
56. Adepoju, T.F. Optimization processes of biodiesel production from pig and neem (*Azadirachta indica* a. Juss) seeds blend oil using alternative catalysts from waste biomass. *Ind. Crops Prod.* **2020**, *149*, 112334. [[CrossRef](#)]
57. Etim, A.O.; Betiku, E.; Ajala, S.O.; Olaniyi, P.J.; Ojumu, T.V. Potential of ripe plantain fruit peels as an ecofriendly catalyst for biodiesel synthesis: Optimization by artificial neural network integrated with genetic algorithm. *Sustainability* **2018**, *10*, 707. [[CrossRef](#)]
58. Srivastava, G.; Paul, A.K.; Goud, V.V. Optimization of non-catalytic transesterification of microalgae oil to biodiesel under supercritical methanol condition. *Energy Convers. Manag.* **2018**, *156*, 269–278. [[CrossRef](#)]
59. Peng, Y.; Parsian, A.; Khodadadi, H.; Akbari, M.; Ghani, K.; Goodarzi, M.; Bach, Q.V. Develop optimal network topology of artificial neural network (AONN) to predict the hybrid nanofluids thermal conductivity according to the empirical data of Al<sub>2</sub>O<sub>3</sub>-Cu nanoparticles dispersed in ethylene glycol. *Phys. A Stat. Mech. Its Appl.* **2020**, *549*, 124015. [[CrossRef](#)]
60. Ghasemi, A.; Hassani, M.; Goodarzi, M.; Afrand, M.; Manafi, S. Appraising influence of COOH-MWCNTs on thermal conductivity of antifreeze using curve fitting and neural network. *Phys. A Stat. Mech. Appl.* **2019**, *514*, 36–45. [[CrossRef](#)]
61. Kumar, S. Comparison of linear regression and artificial neural network technique for prediction of a soybean biodiesel yield. *Energy Sources A Recovery Util. Environ. Eff.* **2020**, *42*, 1425–1435. [[CrossRef](#)]

62. Betiku, E.; Osunleke, A.S.; Odude, V.O.; Bamimore, A.; Oladipo, B.; Okeleye, A.A.; Ishola, N.B. Performance evaluation of adaptive neuro-fuzzy inference system, artificial neural network and response surface methodology in modeling biodiesel synthesis from palm kernel oil by transesterification. *Biofuels* **2021**, *12*, 339–354. [[CrossRef](#)]
63. Sarve, A.; Sonawane, S.S.; Varma, M.N. Ultrasound assisted biodiesel production from sesame (*Sesamum indicum* L.) oil using barium hydroxide as a heterogeneous catalyst: Comparative assessment of prediction abilities between response surface methodology (RSM) and artificial neural network (ANN). *Ultrason. Sonochem.* **2015**, *26*, 218–228. [[CrossRef](#)] [[PubMed](#)]
64. Patel, G.C.M.; Shettigar, A.K.; Parappagoudar, M.B. A systematic approach to model and optimize wear behaviour of castings produced by squeeze casting process. *J. Manuf. Process.* **2018**, *32*, 199–212. [[CrossRef](#)]
65. Zhang, C.; Sun, W.; Wei, H.; Sun, C. Application of artificial intelligence for predicting reaction results in advanced oxidation processes. *Environ. Technol. Innov.* **2021**, *23*, 101550. [[CrossRef](#)]
66. Patel, G.C.M.; Lokare, D.; Chate, G.R.; Parappagoudar, M.B.; Nikhil, R.; Gupta, K. Analysis and optimization of surface quality while machining high strength aluminium alloy. *Measurement* **2020**, *152*, 107337. [[CrossRef](#)]
67. Patel, G.C.; Sibalija, T.V.; Mumtaz, J.; Li, Z. Abrasive water jet machining for a high-quality green composite: The soft computing strategy for modeling and optimization. *J. Braz. Soc. Mech. Sci. Eng.* **2022**, *44*, 83. [[CrossRef](#)]
68. Sibalija, T.V.; Kumar, S.; Patel, G.C.M. A soft computing-based study on WEDM optimization in processing Inconel 625. *Neural Comput. Appl.* **2021**, *33*, 11985–12006. [[CrossRef](#)]
69. Rangappa, R.; Patel, G.C.M.; Chate, G.R.; Lokare, D.; Lakshmikanthan, A.; Giasin, K.; Pimenov, D.Y. Coaxiality error analysis and optimization of cylindrical parts of CNC turning process. *Int. J. Adv. Manuf. Technol.* **2022**, *120*, 6617–6634. [[CrossRef](#)]
70. Patel, G.C. Experimental modeling and optimization of surface quality and thrust forces in drilling of high-strength Al 7075 alloy: CRITIC and meta-heuristic algorithms. *J. Braz. Soc. Mech. Sci. Eng.* **2021**, *43*, 244. [[CrossRef](#)]
71. Patel, G.C.M.; Krishna, P.; Parappagoudar, M.B. Squeeze casting process modeling by a conventional statistical regression analysis approach. *Appl. Math. Model.* **2016**, *40*, 6869–6888. [[CrossRef](#)]
72. Chate, G.R.; Patel, G.C.M.; Deshpande, A.S.; Parappagoudar, M.B. Modeling and optimization of furan molding sand system using design of experiments and particle swarm optimization. *Proc. Inst. Mech. Eng. Part E J. Process Mech. Eng.* **2018**, *232*, 579–598. [[CrossRef](#)]
73. Yang, X.S. Firefly algorithm, stochastic test functions and design optimisation. *Int. J. Bio-Inspired Comput.* **2010**, *2*, 78–84. [[CrossRef](#)]
74. Johari, N.F.; Zain, A.M.; Noorfa, M.H.; Udin, A. Firefly algorithm for optimization problem. *Appl. Mech. Mater.* **2013**, *421*, 512–517. [[CrossRef](#)]
75. Deo, R.C.; Ghorbani, M.A.; Samadianfard, S.; Maraseni, T.; Bilgili, M.; Biazar, M. Multi-layer perceptron hybrid model integrated with the firefly optimizer algorithm for windspeed prediction of target site using a limited set of neighboring reference station data. *Renew. Energy* **2018**, *116*, 309–323. [[CrossRef](#)]
76. Yang, X.S. Multiobjective firefly algorithm for continuous optimization. *Eng. Comput.* **2013**, *29*, 175–184. [[CrossRef](#)]
77. Erol, O.K.; Eksin, I. A new optimization method: Big bang–big crunch. *Adv. Eng. Softw.* **2006**, *37*, 106–111. [[CrossRef](#)]
78. Rezaee Jordehi, A. A chaotic-based big bang–big crunch algorithm for solving global optimisation problems. *Neural. Comput. Appl.* **2014**, *25*, 1329–1335. [[CrossRef](#)]
79. Kaveh, A.; Talatahari, S. Size optimization of space trusses using Big Bang–Big Crunch algorithm. *Comput. Struct.* **2009**, *87*, 1129–1140. [[CrossRef](#)]
80. Hatamlou, A.; Abdullah, S.; Hatamlou, M. Data clustering using big bang–big crunch algorithm. In Proceedings of the International Conference on Innovative Computing Technology, Tehran, Iran, 13–15 December 2011; Springer: Berlin/Heidelberg, Germany; pp. 383–388. [[CrossRef](#)]
81. Mirjalili, S.; Mirjalili, S.M.; Lewis, A. Grey wolf optimizer. *Adv. Eng. Softw.* **2014**, *69*, 46–61. [[CrossRef](#)]
82. Rezaei, H.; Bozorg-Haddad, O.; Chu, X. Grey wolf optimization (GWO) algorithm. In *Advanced Optimization by Nature-Inspired Algorithms*; Springer: Singapore, 2018; pp. 81–91. [[CrossRef](#)]
83. Pradhan, M.; Roy, P.K.; Pal, T. Grey wolf optimization applied to economic load dispatch problems. *Int. J. Electr. Power Energy Syst.* **2016**, *83*, 325–334. [[CrossRef](#)]
84. Salgotra, R.; Singh, U.; Sharma, S. On the improvement in grey wolf optimization. *Neural. Comput. Appl.* **2020**, *32*, 3709–3748. [[CrossRef](#)]
85. Ilham, Z.; Saka, S. Two-step supercritical dimethyl carbonate method for biodiesel production from *Jatropha curcas* oil. *Bioresour. Technol.* **2010**, *101*, 2735–2740. [[CrossRef](#)] [[PubMed](#)]
86. Hsiao, M.C.; Liao, P.H.; Lan, N.V.; Hou, S.S. Enhancement of biodiesel production from high-acid-value waste cooking oil via a microwave reactor using a homogeneous alkaline catalyst. *Energies* **2021**, *14*, 437. [[CrossRef](#)]
87. Muro, C.; Escobedo, R.; Spector, L.; Coppinger, R. Wolf-pack (*Canis Lupus*) hunting strategies emerge from simple rules in computational simulations. *Behav. Processes* **2011**, *88*, 192–197. [[CrossRef](#)]
88. Lee, H.V.; Yunus, R.; Juan, J.C.; Taufiq-Yap, Y.H. Process optimization design for jatropha-based biodiesel production using response surface methodology. *Fuel Process. Technol.* **2011**, *92*, 2420–2428. [[CrossRef](#)]
89. Singh, V.; Belova, L.; Singh, B.; Sharma, Y.C. Biodiesel production using a novel heterogeneous catalyst, magnesium zirconate (Mg<sub>2</sub>Zr<sub>5</sub>O<sub>12</sub>): Process optimization through response surface methodology (RSM). *Energy Convers. Manag.* **2018**, *174*, 198–207. [[CrossRef](#)]

90. Khalilpourazari, S.; Khalilpourazary, S. Optimization of production time in the multi-pass milling process via a Robust Grey Wolf Optimizer. *Neural. Comput. Appl.* **2018**, *29*, 1321–1336. [[CrossRef](#)]
91. Belloufi, A.; Assas, M.; Rezgui, I. Intelligent selection of machining parameters in multipass turnings using firefly algorithm. *Model. Simul. Eng.* **2014**, *2014*, 8. [[CrossRef](#)]
92. Yesilyurt, M.K.; Cesur, C.; Aslan, V.; Yilbasi, Z. The production of biodiesel from safflower (*Carthamus tinctorius* L.) oil as a potential feedstock and its usage in compression ignition engine: A comprehensive review. *Renew. Sustain. Energy Rev.* **2020**, *119*, 109574. [[CrossRef](#)]
93. Berchmans, H.J.; Hirata, S. Biodiesel production from crude *Jatropha curcas* L. seed oil with a high content of free fatty acids. *Bioresour. Technol.* **2008**, *99*, 1716–1721. [[CrossRef](#)]
94. Sadaf, S.; Iqbal, J.; Ullah, I.; Bhatti, H.N.; Nouren, S.; Nisar, J.; Iqbal, M. Biodiesel production from waste cooking oil: An efficient technique to convert waste into biodiesel. *Sustain. Cities Soc.* **2018**, *41*, 220–226. [[CrossRef](#)]
95. Santya, G.; Maheswaran, T.; Yee, K.F. Optimization of biodiesel production from high free fatty acid river catfish oil (*Pangasius hypophthalmus*) and waste cooking oil catalyzed by waste chicken egg shells derived catalyst. *SN Appl. Sci.* **2019**, *1*, 152. [[CrossRef](#)]
96. Awad, S.; Paraschiv, M.; Geo, V.E.; Tazerout, M. Effect of Free Fatty Acids and Short Chain Alcohols on Conversion of Waste Cooking Oil to Biodiesel. *Int. J. Green Energy* **2014**, *11*, 441–453. [[CrossRef](#)]